Nanoscale Advances

ROYAL SOCIETY OF CHEMISTRY

PAPER

View Article Online
View Journal | View Issue

Cite this: *Nanoscale Adv.*, 2026, **8**, 145

Synthesis of a nano-emulsion of quercetin encapsulated vitamin E conjugated iron oxide nanoparticles for the systemic phyto-preventive effect: characterization and oral cancer application

Merhan N. El-Mansy,[a] Zeyad M. Hamdy,[b] Ahmed E. Abdelsamie[bc] and Ola M. El-Borady *[d]

Background: Globally, one of the most pressing public health concerns is the prevention of oral cancerous lesions. This study aimed to reverse the carcinogenic effect of DMBA in hamsters by using nano-emulsions of quercetin encapsulated vitamin E and iron oxide. *Methods:* The studied iron oxide nanoparticles were prepared by the co-precipitation method and then converted into nano-emulsions *via* the oil-in-water technique and characterized. The study included five equal groups of 30 Syrian male hamsters aged eight weeks. Group A constituted a negative control, and Group B received 25 mg kg^{-1} of nano-emulsion orally three times per week for eight weeks. Group C (positive control) was painted with DMBA on the left pouches three times per week for six weeks. Group D received 25 mg kg^{-1} of quercetin thrice per week for two weeks orally, with a continued painting of DMBA per week for six weeks. Group E received 25 mg kg^{-1} of nano-emulsion orally, three times per week, for two weeks, and then continued using it with painting DMBA three times per week for six weeks. *Results*: The morphological and chemical characterization of the synthesized emulsions revealed the formation of spherical particles in the nanoscale emulsion. A significant improvement was noted in the nano-emulsion group compared to the DMBA-painted group in multiple biochemical parameters, such as hemoglobin, RBCs, platelets, WBCs, neutrophils, lymphocytes, monocytes, ALT, AST, creatinine, and urea. The histopathological and immunohistochemical assessments revealed well-differentiated squamous cell carcinoma in the DMBA-treated group, with intense expression of Ki-67 and Bcl-2. In the quercetin-treated group, superficial invasion of carcinoma *in situ* was noted with a moderate decrease in the expression of Ki-67 and Bcl-2. Marked improvement was observed in the quercetin nano-emulsion-treated group that showed moderate to severe dysplasia with an obvious decrease in Ki-67 and Bcl-2 expression. *Conclusion*: The study results confirmed that the prepared quercetin-vitamin E-Fe_3O_4 formulations are novel in combining magnetic targeting and antioxidant co-protection nano-emulsions and significantly prevented oral squamous cell carcinoma in hamsters.

Received 3rd June 2025
Accepted 29th October 2025

DOI: 10.1039/d5na00546a

rsc.li/nanoscale-advances

1. Introduction

Premalignant lesions lead to changes in the epithelium with higher potential for malignancy. They include hyperplasia and atypia with a low risk of malignant transformation, whereas dysplasia represents a higher malignant potential. Oral squamous cell carcinoma (OSCC) is the most debilitating disease that negatively affects the quality of a patient's life. It is considered the sixth most common disease globally, with 700 000 new cases diagnosed each year.[1] Despite the advances in different therapeutic modalities, the 5-year survival rate has not changed and remains at about 50%.[2] It is considered a multi-focal disease through initiation, promotion, and progression that is accompanied by multiple genetic alterations.[3]

The buccal pouch of the hamster (HBP) is a well-validated model to recapitulate the multistage progression of oral carcinogenesis in humans which extends from hyperplasia and dysplasia to invasive carcinoma histologically and gene expression changes.[4] It was first suggested in 1954 and modified in 1961.[1] The most accepted induction protocol involves topical application of 0.5% of 7, 12 dimethyl-benz(*a*)anthracene

[a]*Faculty of Dentistry, Suez Canal University, Kilo 4.5 Ring Road., Ismailia, Egypt. E-mail: merhan_elmansy@dent.suez.edu.eg*

[b]*Faculty of Biotechnology, October University for Modern Science and Arts (MSA), 6th October, Giza, Egypt. E-mail: ziadhamdy100@hotmail.com*

[c]*Faculty of Biology, Adam Mickiewicz University, Poland. E-mail: Ahmed.ibrahemm22@gmail.com*

[d]*Institute of Nanoscience and Nanotechnology, Kafrelsheikh University, 33516, Kafr ElSheikh, Egypt. E-mail: olachem_elborady@yahoo.com; ola_elborady@nano.kfs.edu.eg*

(DMBA) in mineral oil, three times per week, for 8–14 weeks, which produces premalignant and malignant lesions and has been consistently used in chemoprevention and therapeutic studies.[5] DMBA can be metabolized into electrophilic diol-epoxides and then form harmful compounds through binding to adenine and guanine in DNA.[6]

Chemoprevention aims to prevent, delay, or suppress the incidence of tumors using synthetic or natural bioactive agents. These agents help in impeding DNA damage or blocking the premalignant cell division. Most phytochemicals counteract chemoresistance and cause minimal toxicity.[7] Quercetin, a penta-hydroxy flavone, is present in several fruits, vegetables, and grains. It can induce cell cycle arrest and apoptosis due to its anti-inflammatory, antioxidant, signal transduction pathway and enzymatic activity. Its intake through food supplements might allow a protective bioactive effect.[8] Quercetin has also been shown to stop the growth of several malignancies, including lung, breast, pancreatic, colorectal, ovarian, and prostate cancer.[9]

It's critical to comprehend how quercetin regulates apoptotic and proliferative signaling pathways for successful medication. Both intrinsic (mitochondria-mediated) and extrinsic (non-mitochondria-mediated) processes can lead to apoptosis. According to Chien *et al.*[10] quercetin reduced the production of the anti-apoptotic protein Bcl-2. Ki-67 protein expression related to cell proliferation can be used as a biomarker for different histological grades of dysplasia and cancer. The expression of Ki 67 increased according to the severity of oral epithelial dysplasia.[11]

Nanotechnology is the technology of manufacturing materials in the nanoscale range from 1 to 100 nm, which provides new applications in various industries and revolutionizes our lives.[12] Nano-emulsions are colloidal particle systems that act as carriers for particles and are used for several purposes. Magnetic nanoparticles can be utilized to potentiate the effect of the drug delivery system; therefore, the therapeutic efficacy will increase while the side effects and toxic reactions will decrease.[13] Magnetite (Fe_3O_4) nanoparticles could play a vital role in treating cancer. Fe_3O_4 NPs revealed biocompatibility and chemical stability and showed effective photodynamic anti-cancer activity on prostate cancer cell lines.[14] Tween 80 is a common hydrophilic nonionic surfactant used in the emulsification and dispersion of ingredients in pharmaceutical and food products and could be used as a co-emulsifying agent to decrease the size of globules in lipid emulsions and an emulsifying agent in single- and multi-emulsions.[15]

Therefore, this study aimed to evaluate the phyto-preventive efficacy of systemic administration of quercetin and Fe_3O_4 NPs as a nano-emulsion in DMBA-induced dysplasia in the hamster buccal pouch through immunohistochemical detection of Bcl-2 and Ki-67 proteins.

2. Materials and methods

2.1. Preparation of the quercetin nano-emulsion

Firstly, the iron oxide nanoparticles (Fe_3O_4 NPs) were prepared by the co-precipitation method.[16] Quercetin-encapsulated vitamin E-conjugated iron oxide nanoparticles were prepared using the oil-in-water (O/W) nano-emulsion technique, while Tween 80 (MERCK, Germany) was used as an emulsifier and surfactant. Initially, the oil phase was constructed by dissolving 375 mg of quercetin powder (Sigma-Aldrich, Missouri, United States) in 5 ml of absolute ethanol, followed by adding 0.75 g of Tween 80 and 1.5 g of vitamin E; the components were mixed thoroughly by shaking. Secondly, the aqueous phase was prepared by dispersing 0.15 mg Fe_3O_4 NPs in 150 ml of distilled water using a water bath sonicator for one hour.[17] The nano-emulsion was fabricated by slowly dropping the oil phase into the aqueous phase, and the mixture was further pulse-sonicated for 20 min in an ice bath (pulse on, 20.0 s; pulse off, 10.0 s) using a Vibra cell™ ultrasonicator (Newton, Massachusetts, USA) adjusted to 20 000 Hz at room temperature. After sonication, the organic solvent was evaporated by gentle stirring at room temperature. The final nano-emulsion was stored in a refrigerator for further use.

2.2. Nano-emulsion characterization

The particle size and other morphological properties of the nano-emulsion particles were studied using a high-resolution transmission electron microscope (HR-TEM) model JOEL JEM-2010 (Tokyo, Japan) operating at an accelerating voltage of 200 kV. The NPS solution was drop-cast onto TEM grids for the analysis. The lyophilized powder of the nano-emulsion was subjected to XRD examination using an X-ray diffractometer (XRD-6000 Shimadzu) at 40 kV and current regulation at 30 mA with Cu Kα_1 radiation wavelength $\lambda = 1.54056$ Å and an angle range of 10° to 80°. Malvern Zeta-sizer model Nano ZS-90 (Malvern, United Kingdom) operating at 25 °C was used to measure the nano-emulsion potential. To demonstrate the structural compositions of the NPs, Fourier-transform infrared (FTIR) spectra were obtained, and the analysis was attempted using a JASCO spectrometer (Tokyo, Japan) in a scanning range of 4000–400 cm^{-1} using KBr as a reference. The NP sample was dried and mixed with KBr and then compressed into a disc. The UV-vis absorption spectrum of the nano-emulsion in the wavelength range of 200–800 nm was measured using a UV-visible spectrophotometer (V-630 UV–Vis Jasco, Japan). The magnetization M-H hysteresis loop of the powdered samples was collected at room temperature, using a Vibrating Sample Magnetometer (VSM, Lake Shore) from −20 000 to 20 000 Oe.

2.3. Experimental design

Thirty male Syrian golden hamsters (*Mesocricetus auratus*) weighing 90–100 grams were purchased from VACSERA, Giza, Egypt. Animals were housed (six per cage) at a controlled temperature and given water *ad libitum* and nutrients recommended by the regulations of the ethics committee. The drugs were administered through oral gavage, and they were divided into five groups, six per each group as follows: Group A (negative control) did not receive any treatment. Group B (self-negative control) received a quercetin nano-emulsion of 25 mg kg^{-1} orally thrice weekly for eight weeks. Group C (positive control) was painted with DMBA three times weekly on the left pouches

using a paintbrush for six weeks. Group D received a quercetin dose of 25 mg kg^{-1} orally three times per week for two weeks and then continued using it with painting DMBA three times weekly for six weeks. Group E (nanochemo-preventive group) received a quercetin nano-emulsion of 25 mg kg^{-1} orally three times per week for two weeks and then continued using it with painting DMBA three times per week for six weeks.[18]

2.4. Blood sample collection

The animals were anesthetized with cotton-soaked diethyl ether. Blood samples were collected into heparinized capillary tubes to detect a complete blood picture using the kit (Bio-Merieux, Marcy-l'Étoile, France). Blood samples were sent to the Hyah Hematology Laboratory, Egypt. Counting procedures were performed using a fully automatic cell counter (Heco Serc, Italy).

Toxicity enzymes were measured to ensure the safety of the drugs used. Another blood sample was withdrawn into sterile tubes, left to clot at room temperature, and centrifuged at 3000 rpm for 15 min. Serum samples were collected into Eppendorf tubes ready to use or stored at −20 °C. For liver tests, aspartate aminotransferase (AST; catalog # 260001) and alanine aminotransferase (ALT; catalog # 264001) were purchased from the Egyptian Spectrum Diagnostics company for biotechnology (Obour, Egypt). For kidney tests, creatinine (CREAT; catalog # E4370-100) and urea (UR; catalog #K375-100) were purchased from BioVision Company (Milpitas, United States). Every step of the analysis was carried out in compliance with the manufacturer's instructions.

2.5. Histopathological assessment

After the euthanasia of animals with cotton soaked with a lethal dose of diethyl ether, all pouches were fixed in a 10% neutral formalin solution, processed, embedded in soft paraffin, allowed to harden, sectioned into 5 μm using a rotary microtome, mounted on glass slides, and stained with hematoxylin and eosin (H & E) stain for light microscopic study. Two pathologists diagnosed and photographed the slides with an E-330 Olympus digital camera. Epithelial dysplasia (ED) was graded according to Banoczy and Sciba (1976) into mild (limited to the lower third), moderate (extended to the lower two thirds), and severe (extended all over epithelial thickness). Signs of dysplasia might include loss of polarity of basal cells, drop-shaped rete ridges, an increased nuclear–cytoplasmic ratio, hyperchromatism, nuclear pleomorphism, and abnormal mitotic figures. Due to the thin nature of HBP, ED was modified by El-Dakhakhny *et al.*[19] according to the number of signs of dysplasia into mild (two criteria), moderate (3 to 7 criteria), severe (more than 7), and carcinoma *in situ* (top to bottom).

2.6. Immunohistochemical assessment (IHC)

Sections of 5 μm were cut and mounted on positively charged slides to immunohistochemically detect protein expression. Immunostaining was performed using rabbit polyclonal mouse antibody against Ki-67 (Cat. No. RB-1510) with brown nuclear expression as a proliferative marker that provided an indication of dysplastic activity. Another rabbit polyclonal mouse antibody to Bcl-2 (antiapoptotic marker) was purchased from Gene Tex International Corporation, Cat. No. GTX100064, with brown cytoplasmic expression; its overexpression is considered an indicator of resistance to apoptosis. IHC was performed according to the manufacturer's instructions. The computer system utilized was an image analyzer (ImageJ/Fiji 1.46). The area of the screen was measured by digitizing the slides at 400× objective magnification. The software was used to calculate the positive index to assess the area percentage of positive cells through counting the number of immune-positive cells against Ki-67 & Bcl-2 and the number of remaining unstained cells and then calculating the fraction of positive cells for each marker.

2.7. Statistical analysis

All data were collected, calculated, tabulated, and statistically analyzed using the following statistical tests: a normality test (Kolmogorov–Smirnov) to check the normal distribution of the samples, an unpaired sample *T*-test to compare the two groups, and a one-way ANOVA to compare the two groups in each test. Duncan's post hoc test was performed to evaluate statistical significance among the groups. Descriptive statistics were calculated as the mean ± standard deviation (SD). Statistical significance was defined as a P value ≤ 0.05 that allowed readers to improve the strength of each comparison and enhanced the reliability of the data. The statistical significance is defined as a P value ≤ 0.05. All statistical analysis was performed using the computer program SPSS software for Windows version 26.0 (Statistical Package for Social Science, Armonk, NY: IBM Corp.).

3. Results and discussion

A constant challenge for scientific research constitutes the lower survival rate in the previous five years. Researchers looked for new techniques to treat OSCC due to the ineffectiveness of traditional chemotherapy medications or the risk that may occur from surgery, in addition to the expected side effects.[20] Chemoprevention could be utilized to overcome the drawbacks of conventional therapy and turned into a stand-alone therapy or used to prevent the initiation and promotion of tumors.[21] Phytochemicals such as flavonoids have anti-cancer actions by inhibiting cell proliferation, increasing cancer cell death, and modulating key signaling pathways that are involved in the progression of metastatic spread.[22]

Along with its immune-protective and anti-inflammatory effects, quercetin displayed its antimutagenic properties against different mutagens such as benzo(*a*)pyrene and cyclophosphamide, which might have an obvious role in chemoprevention.[23] George *et al.*[24] found that quercetin could be metabolized easily through the action of tyrosinase enzyme to different metabolites that enhanced the effect of its anticancer activity. Also, it could prevent different types of malignant tumors, such as breast and liver cancer.

Multiple nano-delivery platforms have been manufactured to overcome quercetin's poor aqueous solubility, low oral bioavailability, and rapid metabolism. The present nano-

emulsion formulation offered a true oil-in-water submicron dispersion that improved its solubility and lipophilic flavonoid dissolution rate.[25] Moreover, its stability and cellular uptake were optimized through the precise control of droplet size and interfacial properties. It was suitable for potential clinical translations and flexible co-delivery strategies. Here the nano-emulsion expressed a pragmatic and translationally attractive alternative for several nano-carriers which are suitable for long-term chemoprevention.[26]

3.1. Fe_3O_4 NPs and quercetin nano-emulsion characterization

The transmission electron microscopy (TEM) image of the synthesized Fe_3O_4 NPs (Fig. 1A) showed the formation of small-sized NPs, which were mainly spherical in shape and uniformly distributed. The average particle size is approximately 15 nm. Additionally, the selected area electron diffraction (SAED) patterns (inset Fig. 1A) prove the crystalline nature of NPs. In contrast, the TEM image of the quercetin nano-emulsion (Fig. 2A) showed spherical particles with a size of approximately 50 nm, and other semi-spherical shapes within 80–100 nm were detected. The bright areas in the TEM image show quercetin particles, while the dark regions represent Fe_3O_4 NPs. Moreover, the bright spots that appeared in the SAED pattern of the quercetin nano-emulsion (inset Fig. 2A) indicated the presence of iron crystals in the emulsion matrix. Recently, according to TEM images, Chen *et al.*[27] confirmed that the quercetin nanocomposite had a spherical shape with uniform particles, whose sizes ranged from 60 to 70 nm.

Fourier-transform infrared (FTIR) spectroscopy was performed for quercetin, Fe_3O_4NPs, and quercetin nano-emulsion. The FTIR spectrum of Fe_3O_4 NPs (Fig. 1B) showed four main peaks at 3400 cm^{-1}, 1626 cm^{-1}, 885 cm^{-1}, and 572 cm^{-1} corresponding to ν-OH stretching vibrations and the adsorbed water, δ-OH, and Fe–O stretching mode of the tetrahedral and octahedral sites.[28] However, the FTIR spectrum of the pure quercetin (Fig. 2 SI) showed peaks that appeared at around 3405 cm^{-1}, 2923 cm^{-1}, 1665 cm^{-1}, and 1614 cm^{-1}, corresponding to OH groups, =C–H stretch, conjugate C=O, and aromatic C=C stretch, while the peaks in the range from 1451

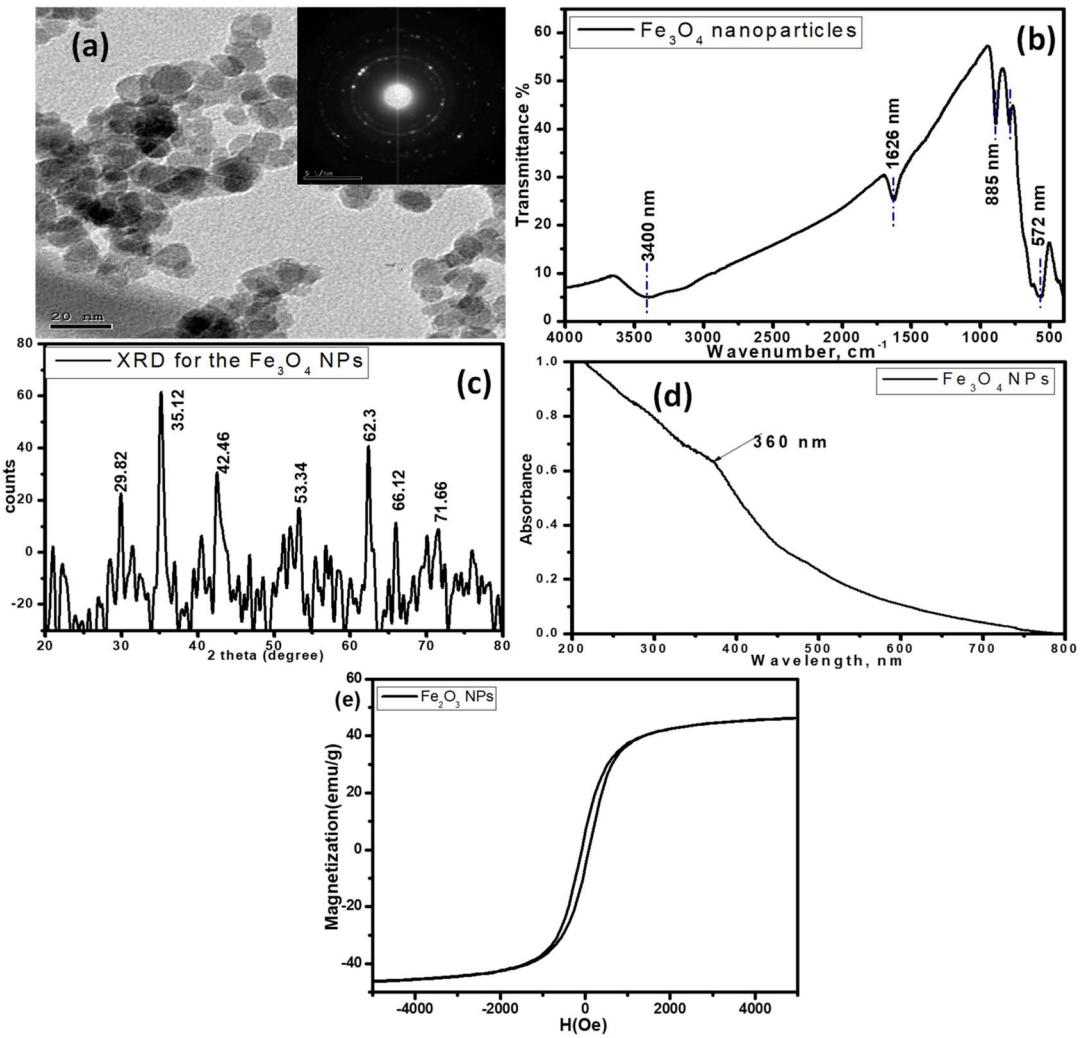

Fig. 1 The characterization of the synthesized Fe_3O_4 NPs, (a) representative TEM image (the inset shows their selected area electron diffraction patterns), (b) the FTIR spectrum, (c) the XRD pattern, (d) the UV-vis absorption spectrum and (e) hysteresis loop (VSM graph) of Fe_3O_4.

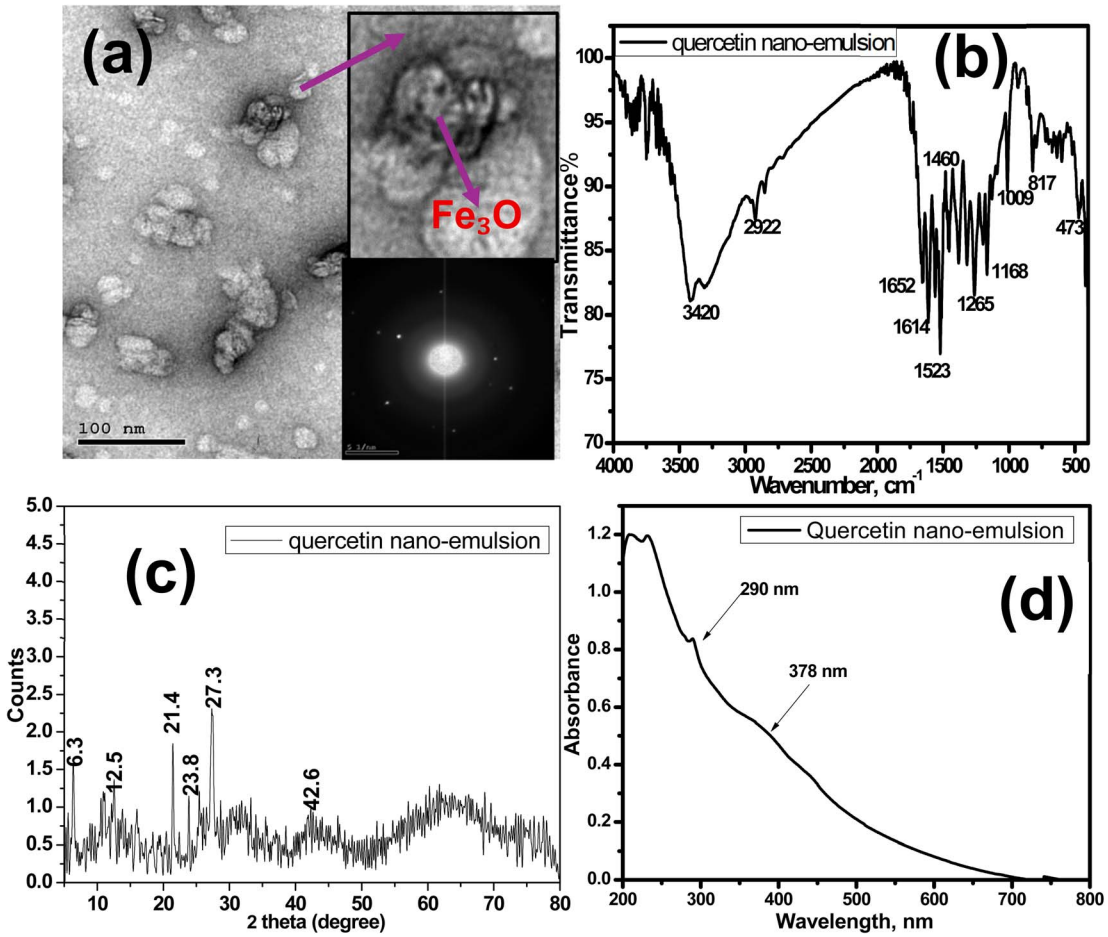

Fig. 2 The characterization of quercetin nano-emulsion encapsulated vitamin E conjugated Fe_3O_4 NPs, (a) representative TEM image (the inset shows its selected area electron diffraction patterns), (b) the FTIR spectrum, (c) the XRD pattern and (d) the UV-vis absorption spectrum.

to 821 cm^{-1} refer to the C–H bending, and C–O stretching covers the region from 1011–1170 cm^{-1}.

In contrast, the FTIR spectrum of the quercetin nano-emulsion (Fig. 2B) showed characteristic bands, demonstrating the effective conjugation of quercetin to iron oxides. Some of these peaks have a broad peak at 3420 cm^{-1} due to the –OH stretching vibration and the Fe–O vibration frequency of the magnetite spinel structure, confirmed by the presence of an absorption band at 473 cm^{-1}, the peak centered at 1652 cm^{-1} assigned to the C═O absorption, and the peaks in the region 1168–1009 cm^{-1} corresponding to C–O stretching. The presence of a peak at 473 cm^{-1} in the FTIR spectrum of the nano-emulsion, which refers to the Fe–O vibration frequency, confirms the existence of Fe_3O_4 NPs in the matrix of quercetin. Moreover, the change in the peak position of some functional groups (OH and C–O groups) in the nano-emulsion compared to pure quercetin indicated its change from pure to nano-form.

X-ray diffraction (XRD) was used to evaluate the crystallinity and structure of Fe_3O_4 NPs, pure quercetin, and quercetin nano-emulsion loaded Fe_3O_4 NPs. The XRD pattern of Fe_3O_4 NPs (Fig. 1C) revealed the appearance of significant peaks at 2θ = 29.82°, 35.12°, 42.46°, 53.34°, 62.3°, 66.12°, and 71.66°, which were previously identified as the crystalline cubic spinel-structured lattice of Fe_3O_4 NPs. Furthermore, the XRD pattern of pure quercetin (Fig. 2, SI) has several strong, distinct peaks that are characteristic of quercetin at 10.8°, 12.5°, 24.1°, 27.3°, and 38.6°. On the other hand, the XRD pattern of the nano-emulsion (Fig. 2C) showed peaks significant for both the Fe_3O_4 NPs and quercetin (2θ = 6.3°, 12.5°, 21.4°, 23.8°, 27.3°, and 42.6°), which confirms the presence of the Fe_3O_4 NPs that emerged with the emulsion, and additional Fe_3O_4 NPs' peaks in the XRD pattern of the nano-emulsion disappeared, which is attributed to breaking the crystallinity of NPs caused by involving the organic structure of quercetin.[29] The X-ray diffraction (XRD) results are consistent with those previously reported by Amanzadeh *et al.*[30]

The electric charges produced at the nanoparticle surface that maintain the stability of NPs were measured using the zeta potential. The zeta potential of the quercetin nano-emulsion prepared in this study is −54.6 mV (Fig. 3, SI). This high value, which represents the great stability of the produced nano-emulsion, may be explained by the surfactant's inclusion of several functional groups into Fe_3O_4 NPs, such as the OH-functional group derived from the quercetin molecule.

The zeta potential offered crucial information on the stability of the quercetin emulsion. According to Tran and his

Fig. 3 Gross appearance of self-control & negative control groups (A), DMBA group (B), quercetin group (C) and nano-emulsion group (D).

colleagues[31] quercetin-containing nano-emulsions had a zeta potential of 26.3 mV, which was probably caused by the presence of castor oil in them. Higher zeta potential values promoted stability by preventing the aggregation of similarly charged particles by repulsive forces between them. In addition to the presence of quercetin, the stabilizer used for fabricating the current nano-emulsions, Tween 80, created a barrier of protection around nanoparticles that persisted on their surface producing high zeta potential (−54.6 mV).

The absorption spectrum of the presented Fe_3O_4 NPs (Fig. 1D) showed a hump-like peak at 360 nm that is characteristic for Fe_3O_4 NPs. Moreover, the absorption spectrum of the nano-emulsion showed two weak absorption bands at 290 nm and 378 nm (Fig. 2D). In UV-vis spectroscopy, the resulting bands were very close to those in other studies about quercetin [32] that validated the effective conjugation of quercetin on the superparamagnetic Fe_3O_4 NPs.[30]

The magnetic behavior of the prepared Fe_3O_4 NPs was examined using vibrating sample magnetometry (VSM). The obtained profile of the Fe_3O_4 NPs (Fig. 2E) exhibits a typical S-shaped hysteresis loop, which is characteristic of superparamagnetic materials. The curve shows negligible coercivity and remanence, indicating that the magnetic nanoparticles do not retain magnetization after the external magnetic field is removed, making the prepared Fe_3O_4 NPs suitable for targeted drug delivery in some biomedical applications. Nevertheless, it was previously observed[33] that when the particle size is sufficiently small for thermal fluctuations to overcome magnetic anisotropy, superparamagnetism is produced. The saturation magnetization (Ms) of the prepared Fe_3O_4 NPs reached approximately 48.563 emu per g, which is consistent with previously reported values for Fe_3O_4 NPs prepared *via* chemical routes.[33–35] This high M_s value suggests that the nanoparticles possess a well-defined crystalline structure and efficient magnetic response.

3.2. Biochemical analysis

As shown from the statistical significance in Table 1, there was no discernible difference between groups (A and B) for the variable examined utilizing the unpaired sample *T*-test at $P < 0.05$. There was a noticeable difference between the four groups (A, C, D and E) for all the examined variables using a one-way ANOVA (*F*-test) at $P < 0.05$. There was a marked decrease in group C, which was treated with DMBA, in hemoglobin (8.9 ± 1.2), RBCs (3622.0 ± 98.9), platelets (318.0 ± 85.3), WBCs (23.8 ± 1.8), neutrophils (5.2 ± 1.5), lymphocytes (93.2 ± 11.6), monocytes (8.2 ± 1.2), ALT (32.1 ± 15.9), AST (46.7 ± 9.4), creatinine (5.1 ± 1.9), and urea (2.5 ± 1.0) in comparison with group A. A slight improvement was noticed in group D treated with quercetin only in comparison with group A as listed in Table 1: 11.1 ± 0.3, 4480.8 ± 78.4, 370.5 ± 70.4, 19.1 ± 3.4, 4.4 ± 1.9, 88.8 ± 32.7, 6.1 ± 1.1, 35.1 ± 17.2, 45.9 ± 11.2, 5.2 ± 1.2, and 3.4 ± 1.8 respectively. After treatment with the nano-emulsion in group E, there was an obvious improvement near

Table 1 Statistical analysis of biochemical results in different groups[a]

	Group A	Group B	Group C	Group D	Group E	F test
HB	16.3 ± 3.2^{a}	15.3 ± 2.1^{a}	8.9 ± 1.2^{c}	11.1 ± 0.3^{b}	12.2 ± 0.9^{b}	29.3
RBCs × 10^3	8090.0 ± 88.1^{a}	8066.0 ± 69.5^{a}	3622.0 ± 98.9^{d}	4480.8 ± 78.4^{c}	6584.0 ± 78.4^{b}	19.5
Platelets × 10^3	540.0 ± 43.8^{a}	522.0 ± 35.9^{a}	318.0 ± 85.3^{d}	370.5 ± 70.4^{c}	450.0 ± 64.2^{b}	9.3
WBCs × 10^3	10.3 ± 2.8^{c}	10.1 ± 3.1^{c}	23.8 ± 1.8^{a}	19.1 ± 3.4^{b}	7.8 ± 1.9^{d}	19.1
Neutrophils	2.0 ± 0.9^{d}	1.6 ± 1.1^{d}	5.2 ± 1.5^{a}	4.4 ± 1.9^{b}	2.8 ± 0.4^{c}	5.9
Lymphocytes	87.0 ± 23.1^{b}	87.0 ± 26.8^{b}	93.2 ± 11.6^{a}	88.8 ± 32.7^{b}	85.2 ± 13.7^{c}	11.4
Monocytes	2.2 ± 0.4^{d}	2.0 ± 0.8^{d}	8.2 ± 1.2^{a}	6.1 ± 1.1^{b}	3.0 ± 0.7^{c}	45.1
ALT	62.6 ± 24.3^{a}	69.0 ± 12.6^{a}	32.1 ± 15.9^{c}	35.1 ± 17.2^{c}	43.7 ± 11.2^{b}	40.1
AST	67.1 ± 12.9^{a}	72.1 ± 13.9^{a}	46.7 ± 9.4^{c}	45.9 ± 11.2^{c}	54.1 ± 6.8^{b}	33.8
Creatinine	18.9 ± 3.8^{a}	23.3 ± 4.5^{a}	5.1 ± 1.9^{c}	5.2 ± 1.2^{c}	14.7 ± 2.3^{b}	16.9
Urea	13.6 ± 1.1^{a}	14.1 ± 3.1^{a}	2.5 ± 1.0^{d}	3.4 ± 1.8^{c}	9.4 ± 0.9^{b}	23.2

[a] a–d: different letters in the same row mean significant differences between groups (at $P < 0.05$).

normal compared to group A in all biochemical parameters: 12.2 ± 0.9, 6584.0 ± 78.4, 450.0 ± 64.2, 7.8 ± 1.9, 2.8 ± 0.4, 85.2 ± 13.7, 3.0 ± 0.7, 43.7 ± 11.2, 54.1 ± 6.8, 14.7 ± 2.3, and 9.4 ± 0.9, respectively.

Consistent with our clinical results, Elmansy *et al.*[36] reported that while using nano-thymoquinone in DMBA-induced carcinogenesis in HBP, there was marked improvement compared to the DMBA-treated group. Moreover, a more immune-enhancing effect was pronounced, through a significant improvement in different biochemical markers. Hao *et al.*[37] demonstrated that in cancer patients, there was a marked thrombocytopenia that led to severe bleeding, the presence of anemia, and a high number of WBCs, including lymphocytes and neutrophils, which indicated an inflammatory response.

In line with our results, Pandya *et al.*[38] documented that urea and creatinine levels indicated impaired renal function due to exposure to toxic materials. Rapid increases in AST and ALT values are a common sign of hepatic toxicity and liver damage, as found in the group painted with DMBA only. As suggested by Jagatheesh *et al.*[39] it may be caused by altered membrane permeability and enzyme leakage from the tissue. Using the quercetin nano-emulsion resulted in a noticeable improvement in liver functions. This conclusion was in line with the findings of Abou Zaid *et al.*[40] who discovered that N-acetyl nano-composite therapy significantly improved DMBA-induced breast carcinomas' high levels of liver enzymes.

3.3. Clinical analysis

Researchers have relied on the HBP model due to its similarity with human OSCC through stepwise clinical, biological, and histological progression. There were matching results between the negative control and self-control groups that showed any alterations in their appearance. The animals appeared healthy throughout the investigation, with regular hair and no skin outbreaks. Also, the length and color of the buccal pouches were normal which revealed enhanced therapeutic effects (Fig. 3A). In contrast, the positive control group displayed observable hair loss, skin ulcers, or abscesses around the oral cavity. All animals were debilitated. The left pouch was shortened. Nodular lesions of various sizes were seen with pronounced blood capillaries (Fig. 3B). These results indicated robust inflammatory reactions which were parallel to the findings in models of chemically induced oral carcinogenesis and necrotic damage.[1] The quercetin group showed smaller multiple lesions compared to group C, with fewer inflammatory signs (Fig. 3C) which are consistent with the findings of Darwish *et al.*[41] who deduced that quercetin reduced tumor incidence. Zhang *et al.*[18] supported our findings which revealed enhanced therapeutic effects with the nano-emulsion group that showed marked recovery with less inflammation. Some animals had tiny lesions, and only a few others had blood capillaries (Fig. 3D).

3.4. Histopathological and immunohistochemical analysis

The mucous membrane in groups A and B showed normal thin keratinized epithelium with no rete ridges, non-inflamed loose connective tissue, and a layer of longitudinally striated muscle, creating deeper C.T. layers (Fig. 4A and B). The immunohistochemical results showed brown nuclear expression of Ki-67 (8.33 ± 0.04) & (10.03 ± 1.04) (Fig. 4C) limited to the basal layer and mild cytoplasmic expression of Bcl-2 (17.49 ± 2.21) & (19.01 ± 3.14) (Fig. 4D).

The left pouches of hamsters painted with DMBA in group C showed well-differentiated squamous cell carcinoma with invading islands of the epithelium into the underlying connective tissue. The dysplastic epithelial cells showed severe alterations, such as drop-shaped rete ridges, an abnormal nuclear/cytoplasmic ratio, cellular and nuclear pleomorphism, basilar hyperplasia, hyperchromatism, and prominent nucleoli (Fig. 4E and F). The basal and supra-basal epithelial layers had widespread, strong nuclear expression of Ki-67, a consequence of the immunohistochemical analysis until the surface of the lesion had statistically significant differences (60.99 ± 8.91) compared with the negative group (8.33 ± 0.04) (Fig. 4G). Also, a significant increase in cytoplasmic expression of Bcl-2 (146.15 ± 24.56) was observed extending all over epithelial thickness (Fig. 4H).

In group D, quercetin was administered orally for two weeks, followed by painting with DMBA for six weeks in conjunction with the administration of quercetin. The results ranged from superficial invasion to carcinoma *in situ*, which had multiple signs of dysplasia (Fig. 5A & B). The IHC data revealed a noticeable decrease in the nuclear expression of Ki-67 (45.22 ± 6.13) compared to the positive control group (60.99 + 8.91), which extended only to most of the epithelial thickness (Fig. 5C). The immunohistochemical analysis demonstrated a reduction in Bcl-2 cytoplasmic expression (112.72 ± 9.11) compared to the (146.15 ± 24.56) positive control group (Fig. 5D).

Endogenous antioxidants could be able to eradicate the free radicals. The performance of the phyto-preventive groups showed marked improvement in the antioxidant system and a significant decrease in the serum malondialdehyde (MDA) level compared to the phyto-therapeutic groups.[42] Following the results of the current study, Zhang *et al.*[18] suggested that quercetin acted as a candidate for oral cancer chemoprevention. Modulation of NF-κB, Bcl-2, and Bax genes in DMBA-induced carcinogenesis declined the severity of dysplasia, reduced the tumor incidence, inhibited cellular proliferation, and induced apoptosis. Consistent with our results, Cheng *et al.*[43] indicated that the anti-inflammatory effect of quercetin was demarcated through the downregulation of intercellular adhesion molecule 1 and matrix metallopeptidase 9. Son and Kim[44] demonstrated that quercetin had different anti-cancer responses against OSCC which repressed cell proliferation with G1 cell cycle arrest and apoptosis by activating the p38 signaling pathway. These findings might provide a new strategy for OSCC therapy using quercetin. In a study by El-Mansy *et al.*,[45] similar histological results were obtained in different groups when using thymoquinone-gold nanoparticles in hamsters to treat OSCC. Alqalshy *et al.*[46] found that hamsters painted with DMBA alone had a high proliferative index by proliferating cell nuclear antigen (PCNA) and Bcl-2 overexpression. Their expression declined after oral administration of docosahexaenoic acid due

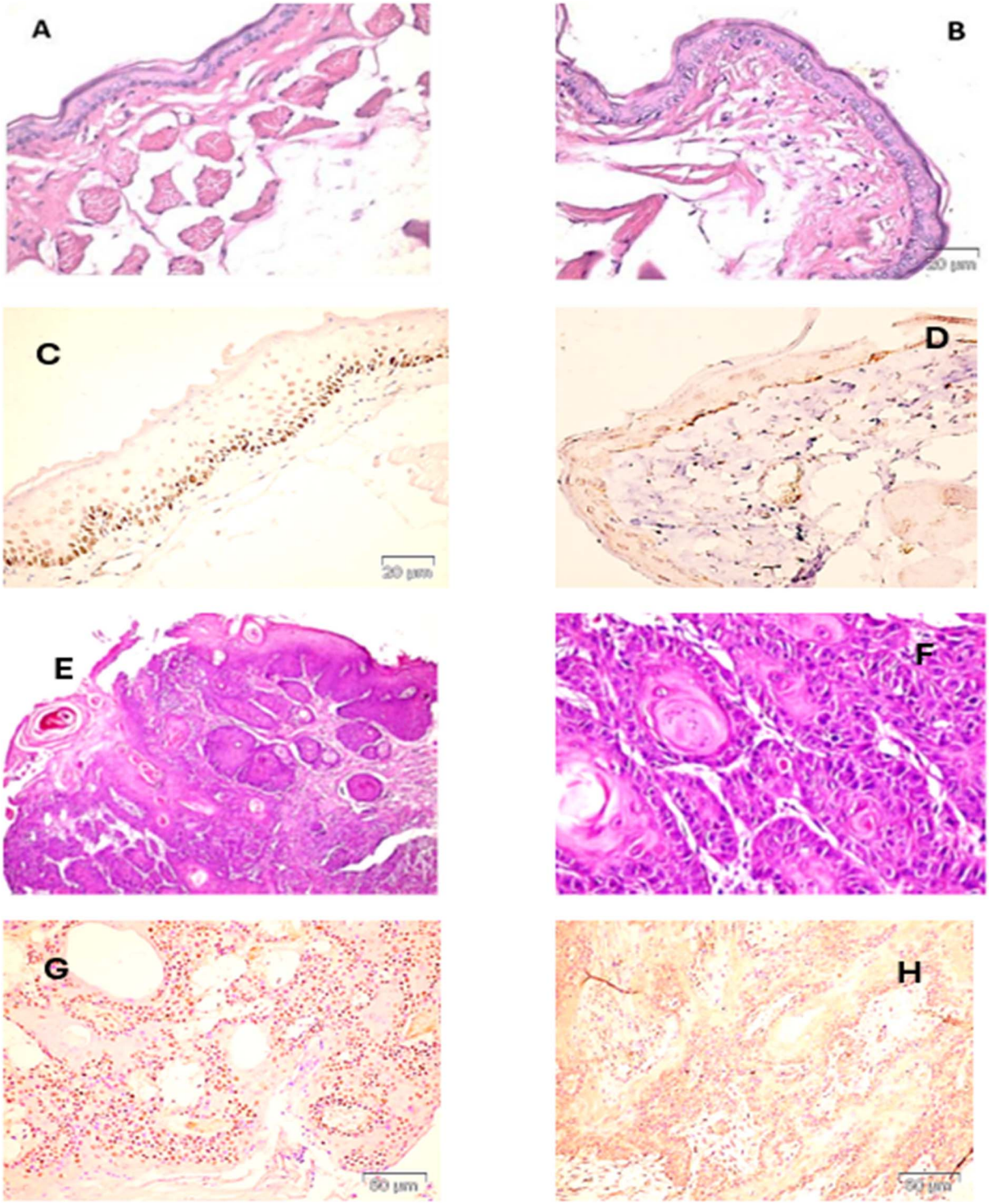

Fig. 4 Photomicrographs showing histological and immunohistochemical expression in control groups. In groups A and B, (A and B) normal histological structure, (C) mild nuclear expression of Ki-67 and (D) mild cytoplasmic expression of Bcl-2. In group C painted with DMBA only, (E and F) well-differentiated squamous cell carcinoma with invading islands of dysplastic epithelium, (G) intense nuclear expression of Ki-67 and (H) intense cytoplasmic expression of Bcl-2.

to its ability to block the initiation or promotion stages of experimentally induced carcinogenesis.

In group E, the same protocol of administration as that for group D was followed using the nano-emulsion instead of quercetin. There was moderate to severe dysplasia, such as basilar hyperplasia, in addition to the observed changes in the nuclear-cytoplasmic ratio, loss of cell polarity of basal cells, and a large nucleolus without invasion of underlying connective tissue (Fig. 5E and F). In contrast to the positive control group (60.99 + 8.91), the IHC results revealed a significantly lower level of nuclear

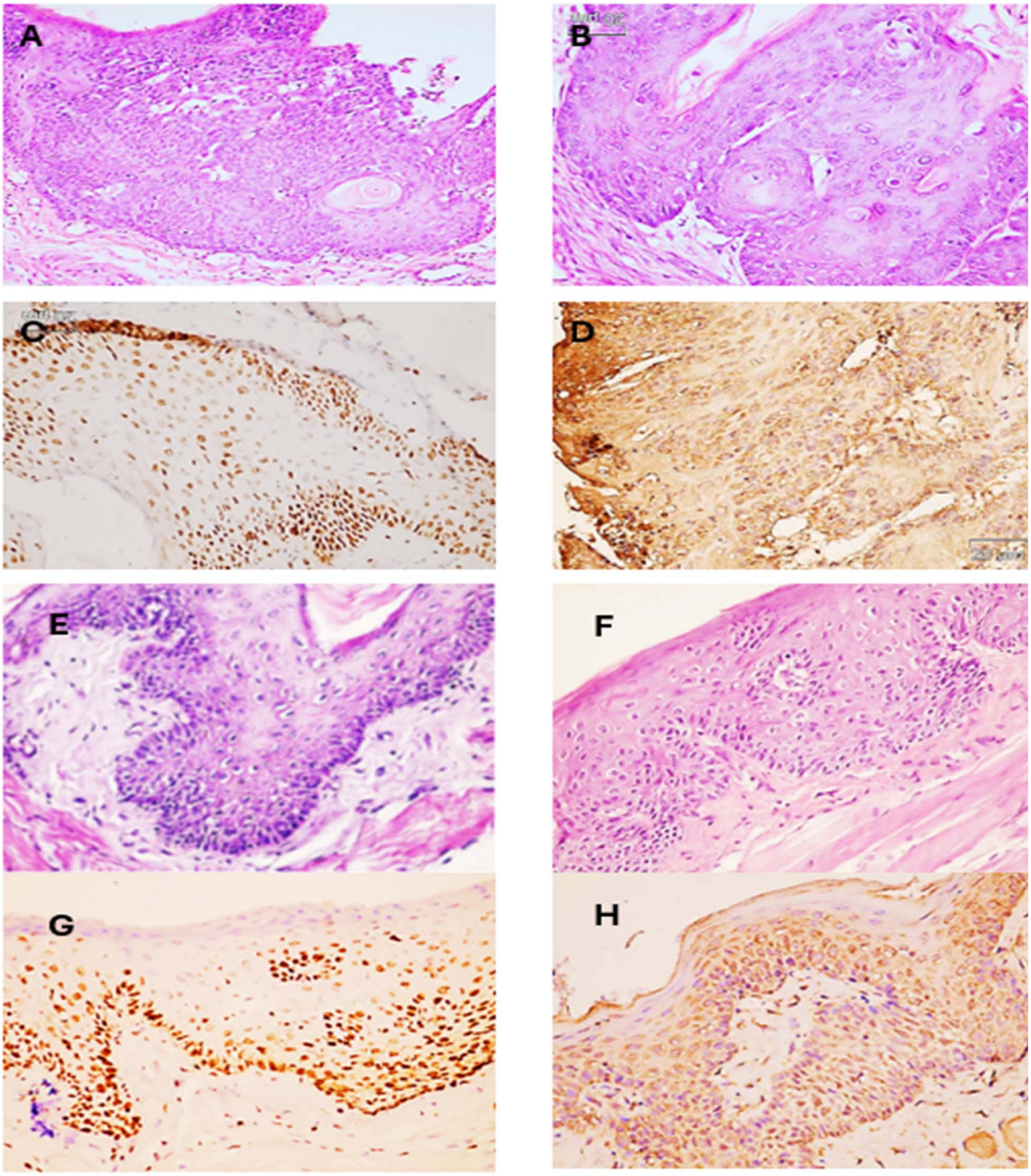

Fig. 5 Photomicrographs showing histological and immunohistochemical expression in treated groups. In group D which received quercetin orally (A and B) superficial invasion to carcinoma *in situ*, (C) a decrease in the nuclear expression of Ki-67 and (D) a reduction in Bcl-2 cytoplasmic expression. In group E which received the nano-emulsion orally, (E and F) moderate to severe dysplasia (G), a significant decrease in the nuclear expression of Ki-67 (H) and a significant reduction in cytoplasmic expression of Bcl-2.

expression of Ki-67 (21.41 + 3.67), which was limited to basal and parabasal layers only (Fig. 5G). Also, it demonstrated a significant reduction in Bcl-2 cytoplasmic expression (65.22 ± 13.24) compared to the (146.15 ± 24.56) positive control group (Fig. 5H).

In the present formulation, vitamin E has a dual functionality where it improved the stability, pharmaceutical properties and mucosal delivery of quercetin. Moreover, its own formula has a chemo-preventive activity. Previous study has demonstrated that it exerted synergistic antioxidant and anti-proliferative effects that suppressed key biomarkers of carcinogenesis including Ki-67 and Bcl-2.[47] Per our results, iron oxide nanoparticles could be effective in tumor treatment. Elmasry *et al.*[48] concluded that quercetin-

conjugated Fe_3O_4 nanoparticles could inhibit cell proliferation with negligible toxicity to normal cells by promoting ROS generation to show their potential therapeutic effect. Another study assumed that quercetin induced programmed cell death in oral cancer cell lines by decreasing the expression of Bcl-2 to induce antineoplastic activity. Mitochondrial de-functionalization increased the leakage of cytochrome c release that activated caspase 3.[49] On the other hand, reactive oxygen species (ROS) could be produced from Fe_3O_4 NPs, which led to the formation of the superhydroxide hydrogen and hydroxyl radicals that could induce apoptosis[50] and used in oncology.[51]

Overall, the incorporation of quercetin into vitamin E–Fe_3O_4 to form a hybrid nanoemulsion provides advantages over other polymeric carriers using conventional methods. The current novel nanoemulsion contains vitamin E, which may improve membrane compatibility and offer antioxidant activity, that can shield quercetin from oxidative degradation and facilitate its integration into lipid environments or cell membranes. Additionally, the presence of Fe_3O_4, which provides a magnetic response, may improve targeting to diseased tissues and decrease the systemic side effects. Therefore, the prepared hybrid nanoemulsion possesses a dual function (antioxidant and magnetic targeting) that many polymeric systems lack or only partially deliver, leading to an increase in bioavailability and cellular uptake compared to other natural polymeric nanocomposites.

4. Limitations and future work

In future work, the authors plan to investigate the molecular mechanisms underlying the observed chemopreventive effects by examining the involvement of oxidative stress, apoptotic, and signaling pathways (such as PI3K/Akt and NF-κB). Moreover, we intend to explore the potential modulation of immune checkpoint molecules (PDL-1 and CTLA-4) to better understand the immunoregulatory aspects contributing to the nano-emulsion's anticancer activity.

5. Conclusion

The current study offered successful fabrication of a quercetin-loaded Fe_3O_4 NP nano-emulsion as confirmed by its morphological and spectral characterization. The quercetin nanoemulsion played an obvious role in the retardation of the transition of oral epithelial dysplasia to oral squamous cell carcinoma, as confirmed by our clinical, biochemical, histological, and immunohistochemical results. It induced apoptosis by minimizing the expression of Bcl-2 and Ki-67 proteins in hamster buccal pouches. Therefore, the quercetin nano-emulsion could be utilized as a good strategy for cancer chemoprevention to minimize the mortality associated with cancerous lesions.

Declarations

Ethics approval

The ethical committee of the Faculty of Dentistry, Suez Canal University, Ismailia, Egypt, has approved the experiment (633/2023).

Author contributions

Conception: M. N. El-Mansy and O. M. El-Borady; formal analysis and investigation: M. N. El-Mansy, Z. M. Hamdy, A. E. Abdelsamie, and O. M. El-Borady; experimental design for nanomaterials: O. M. El-Borady; experimental design for biomedical work: M. N. El-Mansy, Z. M. Hamdy, and A. E. Abdelsamie; supervision and visualization: M. N. El-Mansy and O. M. El-Borady; writing: M. N. El-Mansy, Z. M. Hamdy, A. E. Abdelsamie, and O. M. El-Borady; all authors reviewed the manuscript.

Conflicts of interest

The authors declare that there is no conflict of interest.

Data availability

The datasets supporting the findings of this study will be made publicly available without the need for a request.

Supplementary information is available. See DOI: **https://doi.org/10.1039/d5na00546a**.

Acknowledgements

The authors gratefully acknowledge Prof. Dr Ayman Diab (Faculty Dean) and Prof. Dr Gehan Safwat (Faculty vice Dean) (Faculty of Biotechnology, October University for Modern Sciences & Arts (MSA), Egypt) for their support and encouragement.

References

1 S. Nagini and J. Kowshik, The hamster buccal pouch model of oral carcinogenesis, *Gastrointest. Physiol. Dis. Methods Protoc.*, 2016, 341–50.
2 L. M. Mahakian, D. G. Farwell, H. Zhang, J. W. Seo, B. Poirier, S. P. Tinling, *et al.*, Comparison of PET imaging with 64 Cu-liposomes and 18 F-FDG in the 7,12-dimethylbenz[*a*] anthracene (DMBA)-induced hamster buccal pouch model of oral dysplasia and squamous cell carcinoma, *Mol. Imaging Biol.*, 2014, **16**, 284–92.
3 L. Feller and J. Lemmer, *Oral squamous cell carcinoma: epidemiology, clinical presentation and treatment*. 2012.
4 Z. Wang and R. T. Cormier, Golden Syrian hamster models for cancer research, *Cells*, 2022, **11**, 2395.
5 M. S. Shata, R. H. El-Sherbiny, O. M. El-Borady and M. N. Elmansy, Anti-cancerous Impact of Topical Chitosan Nanoparticles in DMBA-Induced Oral Precancerous Lesions, *Egypt. Dent. J.*, 2025, **71**, 2185–2194.
6 Y.-K. Chen and L.-M. Lin, DMBA-induced hamster buccal pouch carcinoma and VX2-induced rabbit cancer as a model for human oral carcinogenesis, *Expert Rev. Anticancer Ther.*, 2010, **10**, 1485–1496.
7 M. Swetha, C. K. Keerthana, T. P. Rayginia and R. J. Anto, Cancer chemoprevention: A strategic approach using phytochemicals, *Front. Pharmacol*, 2022, **12**, 809308.

8 N. Li and J. Wang, Quercetin induces cytotoxicity and apoptosis, reduces metastasis and drug resistance in oral cancer cells, *Turk. J. Biochem.*, 2024, **49** 156–148 ,(2).
9 A. Vafadar, Z. Shabaninejad, A. Movahedpour, F. Fallahi, M. Taghavipour, Y. Ghasemi, *et al.*, Quercetin and cancer: new insights into its therapeutic effects on ovarian cancer cells, *Cell Biosci.*, 2020, **10**, 1–17.
10 S.-Y. Chien, Y.-C. Wu, J.-G. Chung, J.-S. Yang, H.-F. Lu, M.-F. Tsou, *et al.*, Quercetin-induced apoptosis acts through mitochondrial-and caspase-3-dependent pathways in human breast cancer MDA-MB-231 cells, *Hum. Exp. Toxicol.*, 2009, **28**, 493–503.
11 A. Takkem, C. Barakat, S. Zakaraia, K. Zaid, J. Najmeh, M. Ayoub, *et al.*, Ki-67 prognostic value in different histological grades of oral epithelial dysplasia and oral squamous cell carcinoma, *Asian Pac. J. Cancer Prev.*, 2018, **19**, 3279.
12 S. Bayda, M. Adeel, T. Tuccinardi, M. Cordani and F. Rizzolio, The history of nanoscience and nanotechnology: from chemical–physical applications to nanomedicine, *Molecules*, 2019, **25**, 112.
13 M. Jaiswal, R. Dudhe and P. K. Sharma, Nanoemulsion: an advanced mode of drug delivery system, *3 Biotech.*, 2015, **5**, 123–127.
14 K. C. Nam, K.-H. Choi, K.-D. Lee, J. H. Kim, J.-S. Jung and B. J. Park, Particle size dependent photodynamic anticancer activity of hematoporphyrin-conjugated Fe_3O_4 particles, *J. Nanomater.*, 2016, **2016**, 1.
15 K. Prabhakar, S. M. Afzal, G. Surender and V. Kishan, Tween 80 containing lipid nanoemulsions for delivery of indinavir to brain, *Acta Pharm. Sin. B*, 2013, **3**, 345–353.
16 B. H. Hui, M. N. Salimi. Production of iron oxide nanoparticles by co-precipitation method with optimization studies of processing temperature, pH and stirring rate, in *IOP Conference Series: Materials Science and Engineering*, IOP Publishing, 2020, p. 12036.
17 M. Elsamman, O. M. El-Borady, M. M. Nasr, Z. Al-Amgad and A. A. Metwally, Development of propolis, hyaluronic acid, and vitamin K nano-emulsion for the treatment of second-degree burns in albino rats, *BMC Complementary Med. Ther.*, 2024, **24**, 92.
18 W. Zhang, G. Yin, J. Dai, Y. U. Sun, R. M. Hoffman, Z. Yang, *et al.*, Chemoprevention by quercetin of oral squamous cell carcinoma by suppression of the NF-κB signaling pathway in DMBA-treated hamsters, *Anticancer Res.*, 2017, **37**, 4041–4049.
19 M. El-Dakhakhny, M. A. Hassan and G. Abd El-Aziz, Effect of thymoquinone and poly-thymoqunione on chemicallyinduced oral epithelial dysplasia (experimental study), *Int Acad Res J*, 2009, **1**, 107–117.
20 A. Ranjan, S. Ramachandran, N. Gupta, I. Kaushik, S. Wright, S. Srivastava, *et al.*, Role of phytochemicals in cancer prevention, *Int. J. Mol. Sci.*, 2019, **20**, 4981.
21 Y.-J. Zhang, R.-Y. Gan, S. Li, Y. Zhou, A.-N. Li, D.-P. Xu, *et al.*, Antioxidant phytochemicals for the prevention and treatment of chronic diseases, *Molecules*, 2015, **20**, 21138–21156.
22 A. Liskova, L. Koklesova, M. Samec, K. Smejkal, S. M. Samuel, E. Varghese, *et al.*, Flavonoids in cancer metastasis, *Cancers*, 2020, **12**, 1498.
23 S. Shivakumar, Y. L. Tadakaluru, R. R. R. Yakkanti, S. R. Suresh and C. S. Pasula, Role of Quercetin in chemoprevention against wide range of carcinogens and mutagens, *Int. J. Drug Deliv.*, 2017, **9**, 10–5138.
24 V. C. George, G. Dellaire and H. P. V. Rupasinghe, Plant flavonoids in cancer chemoprevention: role in genome stability, *J. Nutr. Biochem.*, 2017, **45**, 1–14.
25 E.-M. Tomou, P. Papakyriakopoulou, E.-M. Saitani, G. Valsami, N. Pippa and H. Skaltsa, Recent advances in nanoformulations for quercetin delivery, *Pharmaceutics*, 2023, **15**, 1656.
26 H. S. Mahajan and N. D. Patil, Nanoemulsion containing a synergistic combination of curcumin and quercetin for nose-to-brain delivery: In vitro: and: in vivo: studies, *Asian Pac. J. Trop. Biomed.*, 2021, **11**, 510–518.
27 L.-C. Chen, Y.-C. Chen, C.-Y. Su, C.-S. Hong, H.-O. Ho and M.-T. Sheu, Development and characterization of self-assembling lecithin-based mixed polymeric micelles containing quercetin in cancer treatment and an in vivo pharmacokinetic study, *Int. J. Nanomed.*, 2016, 1557–1566.
28 M. Ishii, M. Nakahira and T. Yamanaka, Infrared absorption spectra and cation distributions in (Mn, Fe) 3O4, *Solid State Commun.*, 1972, **11**, 209–212.
29 M. Zare, M. N. Sarkati, H. Tashakkorian and S. Rahaiee, Quercetin immobilization onto Chitosan-Functionalized Fe3O4 magnetic nanoparticles: Biocompatible nanomedicine for overcoming cancer cells, *J. Cluster Sci.*, 2022, **33**, 449–455.
30 E. Amanzadeh, A. Esmaeili, R. E. N. Abadi, N. Kazemipour, Z. Pahlevanneshan and S. Beheshti, Quercetin conjugated with superparamagnetic iron oxide nanoparticles improves learning and memory better than free quercetin via interacting with proteins involved in LTP, *Sci. Rep.*, 2019, **9**, 6876.
31 T. H. Tran, Y. Guo, D. Song, R. S. Bruno and X. Lu, Quercetin-containing self-nanoemulsifying drug delivery system for improving oral bioavailability, *J. Pharm. Sci.*, 2014, **103**, 840–852.
32 L. Forte, P. Torricelli, E. Boanini, M. Gazzano, K. Rubini, M. Fini, *et al.*, Antioxidant and bone repair properties of quercetin-functionalized hydroxyapatite: an in vitro osteoblast–osteoclast–endothelial cell co-culture study, *Acta Biomater.*, 2016, **32**, 298–308.
33 Z. Kelgenbaeva, E. Omurzak, S. Takebe, Z. Abdullaeva, S. Sulaimankulova, C. Iwamoto, *et al.*, Magnetite nanoparticles synthesized using pulsed plasma in liquid, *Jpn. J. Appl. Phys.*, 2013, **52**, 11NJ02.
34 B. S. Corrêa, M. S. Costa, G. A. Cabrera-Pasca, C. Sena, P. R. H. Holanda, A. P. S. Silva, *et al.*, High-saturation magnetization in small nanoparticles of Fe3O4 coated with natural oils, *J. Nanopart. Res.*, 2020, **22**, 68.
35 B. S. Corrêa, M. S. Costa, G. A. Cabrera-Pasca, C. Sena, R. H. Holanda Pinto, A. P. S. Silva, *et al.*, High-saturation

magnetization in small nanoparticles of Fe_3O_4 coated with natural oils, *J. Nanopart. Res.*, 2020, **22**, 1–15.

36 M. N. Elmansy, M. S. S. S. Shata and O. El Borady, Effect of nano-thymoquinone on tumor necrosis factor-α in DMBA-induced hamster buccal pouch carcinogenesis, *Egypt. Dent. J.*, 2020, **66**, 2389–2400.

37 L. Hao, J. Zhang, Y. Di and Z. Tan, Prognostic value of white blood cells detected for the first time after adjuvant chemotherapy in primary operable non-small cell lung cancer, *Technol. Cancer Res. Treat.*, 2018, **17**, 1533033818802813.

38 D. Pandya, A. K. Nagrajappa and K. S. Ravi, Assessment and correlation of urea and creatinine levels in saliva and serum of patients with chronic kidney disease, diabetes and hypertension–a research study, *J. Clin. Diagn. Res.*, 2016, **10**, ZC58.

39 K. Jagatheesh, V. Arumugam, N. Elangovan and P. PavanKumar, Evaluation of the anti-tumor and antioxidant activity of Amorphophallus paeonifolius on DMBA induced mammary carcinoma, *J. Chem. Pharm. Sci.*, 2010, **1**(2), 40–50.

40 O. A. Abou Zaid, A. F. Badawi and S. A. Elsayes, Studies on the chemopreventive potential of N-acetyl cysteine/zinc oxide nanocomposite combined with high ascorbate on 7, 12-dimethylbenz (a) anthracene-induced mammary carcinogenesis in rats, *Int J. Pharma Sci.*, 2015, **5**(2), 976–980.

41 W. M. Darwish, A. S. Abdoon, M. S. Shata and M. Elmansy, Vincristine-loaded polymeric corona around gold nanorods for combination (chemo-photothermal) therapy of oral squamous carcinoma, *React. Funct. Polym.*, 2020, **151**, 104575.

42 M. Lotfi, S. Kazemi, A. Ebrahimpour, F. Shirafkan, M. Pirzadeh, M. Hosseini, *et al.*, Protective effect of quercetin nanoemulsion on 5-fluorouracil-induced oral mucositis in mice, *J. Oncol.*, 2021, **2021**, 1–10.

43 S.-C. Cheng, Y.-H. Wu, W.-C. Huang, J.-H. S. Pang, T.-H. Huang and C.-Y. Cheng, Anti-inflammatory property of quercetin through downregulation of ICAM-1 and MMP-9 in TNF-α-activated retinal pigment epithelial cells, *Cytokine*, 2019, **116**, 48–60.

44 H.-K. Son and D. Kim, Quercetin induces cell cycle arrest and apoptosis in YD10B and YD38 oral squamous cell carcinoma cells, *Asian Pac. J. Cancer Prev.*, 2023, **24**, 283.

45 M. N. El-Mansy, M. M. Hassan, A. El-Nour, M. Kholoud and W. H. El-Hosary, Treatment of oral squamous cell carcinoma using thymoquinone loaded on gold nanoparticles, *Suez Canal Univ. Med. J.*, 2017, **20**, 11–19.

46 E. M. Alqalshy, A. M. Ibrahim, A. A.-S. Abdel-Hafiz, K. A. E.-R. Kamal, M. A. Alazzazi, M. R. Omar, *et al.*, Effect of docosahexaenoic acid as a chemopreventive agent on experimentally induced hamster buccal pouch carcinogenesis, *Cancer Treat Res Commun.*, 2022, **31**, 100558.

47 M. J. Saadh, H. H. Ahmed, M. Chandra, A. F. Al-Hussainy, J. A. Hamid, A. Mishra, *et al.*, Therapeutic effects of quercetin in oral cancer therapy: a systematic review of preclinical evidence focused on oxidative damage, apoptosis and anti-metastasis, *Cancer Cell Int.*, 2025, **25**, 66.

48 S. A. Elmasry, M. A. Elgawish, O. E. El-Shawy, M. A. Askar, E. A. Helmy and L. A. Rashed, Biologically synthesized Quercetin loaded magnetite nanoparticles enhanced cytotoxicity and radiosensitivity of cancer cells in Vitro, *J. Chem. Pharm. Res.*, 2016, **8**, 758–771.

49 Y. Ma, C. Yao, H. Liu, F. Yu, J. Lin, K. Lu, *et al.*, Quercetin induced apoptosis of human oral cancer SAS cells through mitochondria and endoplasmic reticulum mediated signaling pathways, *Oncol. Lett.*, 2018, **15**, 9663–9672.

50 M. I. Khan, A. Mohammad, G. Patil, S. A. H. Naqvi, L. K. S. Chauhan and I. Ahmad, Induction of ROS, mitochondrial damage and autophagy in lung epithelial cancer cells by iron oxide nanoparticles, *Biomaterials*, 2012, **33**, 1477–1488.

51 H. Wang, L. Hu, J. Du, L. Peng, L. Ma and Y. Zhang, Development of rheologically stable high internal phase emulsions by gelatin/chitooligosaccharide mixtures and food application, *Food Hydrocoll.*, 2021, **121**, 107050.